ISSN (O): 2320-5407
ISSN (P): 3107-4928

Journal Homepage: -www.journalijar.com

INTERNATIONAL JOURNAL OF ADVANCED RESEARCH (IJAR)

Article DOI: 10.21474/IJAR01/23772
DOI URL: http://dx.doi.org/10.21474/IJAR01/23772

RESEARCH ARTICLE

INTERPLANETARY CHARACTERISTICS AND GEOEFFECTIVENESS DURING RECURRENT GEOMAGNETIC ACTIVITIESOF THE SOLAR CYCLES 23 AND 24

Diabate Abidina[1,4,5], Gyebre Aristide Marie Frederic[2,5], Bassoleth Jean Valentin[5], Guibula Karim[3,5], Zerbo Jean Louis[1,4,5] and Ouattara Frederic[2,5]

1. Universite Nazi Boni (UNB), Bobo-Dioulasso, Burkina Faso.
2. Université Norbert ZONGO (UNZ), Koudougou, Burkina Faso.
3. Université Virtuelle du Burkina Faso (UV-BF).
4. Laboratoire de Matériaux, d'Heliophysique et Environnement (La.M.H.E), Burkina Faso.
5. Laboratoire de Chimie Analytique, de Physique Spatiale et Énergétique (L@CAPSE), Burkina Faso.

……………………………………………………………………………………………………....

Manuscript Info

……………………….

Manuscript History
Received: 08 May 2026
Final Accepted: 10 June 2026
Published: July 2026

Abstract

………………………………………………………………

Recurrent geomagnetic activity represents an important component of solar-terrestrial interactions and is mainly associated with high-speed solar wind streams originating from long-lived coronal holes.This study aims to investigate the interplanetary characteristics and geoeffectivene ss of this type of activity observed during solar cycles 23 and 24 (1996-2019). Twenty-eight (28) recurrent geomagnetic events were identified using the Aa index and the Sudden Storm Commencement (SSC) dates. Solar wind parameters (speed, proton density, dynamic pressure, and IMF Bz component) and the Dst index were investigated through individual-event analysis, Superposed Epoch Analysis (SEA), and correlation analysis. The individual-event analysis showed that 26 of the 28 events share common interplanetary signatures that are consisten tly reproduced by the SEA composite profiles.These analyses reveal the typical SIR/CIR signature, characterized by a progressive increase in solar wind speed, early enhancements in proton density and dynamic pressure, recurrent southward IMF Bz intervals, and a decrease in Dst reaching weak-to-moderate storm levels.Correlation analyses further highlight the temporal relationships between interplanetary parameters and geomagnetic activity: solar wind speed acts as a precursor of geom agnetic activity, while the IMF Bz component has a more direct influen ce on the development of geomagnetic storms through the reconnection phenomenon. Proton density and dynamic pressure modulate the intensi ty of the magnetospheric response during the principal phase.

……………………………………………………………………………………………………....

These findings strengthen the understanding of the interplanetary processes controlling the geoeffectiveness of recurrent geomagnetic events and contribute to an improved physical interpretation of these events, with potential applications for space weather forecasting.

Corresponding Author:-Diabate Abidina
Address:-1. Universite Nazi Boni (UNB), Bobo-Dioulasso, Burkina Faso.4. Laboratoire de Matériaux, d'Heliophysique et Environnement (La.M.H.E), Burkina Faso.5. Laboratoire de ChimieAnalytique, de Physique Spatiale et Énergétique (L@CAPSE), Burkina Faso.

Introduction:-

For over a century, researchers have investigated Earth's magnetic field, its perturbations, and the sources of these perturbations. Early studies by (1), (2) and (3) established the foundations of modern geomagnetism by demonstrating that geomagnetic variations are linked to solar activity. These discoveries transformed geomagnetism from a purely terrestrial discipline into a solar-terrestrial science and paved the way for modern space weather research.

Modern space weather research has shown that most geomagnetic disturbances can be linked to specific solar and interplanetary phenomena, including sunspots, coronal mass ejections, and solar wind structures (4). Thus, the work of (5) and (6), based on a statistical analysis of over a century of data (1868–1978) directly related to solar phenomena and utilizing the geomagnetic index Aa established by (7), laid the foundations for the classification of geomagnetic activities. They distinguished four main classes: (a) quiet activity related to normal solar wind conditions and characterized by weak geomagnetic perturbation, (b) shock activity caused by coronal mass ejections (CMEs), (c) recurrent activity associated with high-speed solar wind streams from coronal holes, and (d) fluctuating activity due to irregular variations (fluctuations) in the solar wind during its flow. This classification was later confirmed and refined by several authors, including (8), (9) , (10), thereby contributing to a more robust and standardized classification of geomagnetic activity. (11) refined the classification of (5), (6) using a larger database (1868 – 2009) and taking into account the effect of active regions and moderate winds that were embedded in the fluctuating ones. This approach preserved the four-class classification of geomagnetic activity while adjusting the aa-index thresholds and reducing the range of fluctuating activity in favor of recurrent and shock activities. These advances established recurrent geomagnetic activity as a distinct class associated with high-speed solar wind streams originating from coronal holes. However, the interplanetary conditions controlling the geoeffectiveness of these recurrent events remain insufficiently understood, motivating further investigation.

Moreover, the ability of a solar or interplanetary event to produce measurable geomagnetic disturbances on Earth is termed geoeffectiveness (12, 13, 14). Geomagnetic storms, which represent the most significant manifestation of geomagnetic disturbances, are commonly quantified using indices such as Dst (Disturbance storm time), Kp, AE (Auroral Electrojet), SYM-H (15, 16, 17, 18). The Dst index, which is the most widely used indicator of geomagnetic storm intensity, reflects the enhancement of the ring current (15). A decrease in Dst occurs when the interplanetary magnetic field (IMF) is oriented southward and the solar wind speed is high. This promotes magnetic reconnection and the injection of energy into the ring current. Consequently, identifying the interplanetary conditions that control the intensity of geomagnetic disturbances is fundamental to understanding the geoeffectiveness of recurrent geomagnetic events. This scientific context naturally raises the question of which interplanetary signatures are consistently associated with geoeffective recurrent events.

While the solar origin of recurrent geomagnetic events is acknowledged, their interplanetary signatures and geoeffectiveness remain insufficiently characterized. The aim of this study is to identify the interplanetary signatures characteristic of recurrent geomagnetic events and to assess their geoeffectiveness using three complementary approaches: individual-event analysis, Superposed Epoch Analysis (SEA), and correlation analysis. By combining these complementary methods, this study aims to provide a robust and coherent physical interpretation of the interplanetary processes controlling the geoeffectiveness of recurrent geomagnetic events.

Data and Methods:-

Data:-

The present study uses the following datasets:-

- Storm Sudden Commencement (SSC) dates and daily mean values of the geomagnetic Aa index. These data are used to identify days of recurrent geomagnetic activity and are available through the International Service of Geomagnetic Indices (ISGI);
- Solar wind parameters, including solar wind speed, proton density, dynamic pressure, and Bz component of the interplanetary magnetic field expressed in the GSM coordinate system. These parameters were used to characterize the interplanetary conditions associated with recurrent events and to investigate their contribution to geoeffectiveness. The corresponding hourly data are obtained from the OMNI database (18, 20) through the OMNIWeb service;
- HourlyDst index values, which are used to assess the geoeffectiveness of recurrent geomagnetic activity events. Hourly Dst values are also obtained from the OMNIWeb database

Alldatasetscover solar cycles 23 and 24 (1996 – 2019).

Method:-

Identification of recurrent geomagnetic activity days:-

According to (21), recurrent geomagnetic activity results primarily from high-speed solar wind streams originating from long – lived coronal holes and is characterized by a periodicity close to the synodic solar rotation period (~27 days). Subsequent studies, including those of (9) and (10), confirmed this definition and further refined the criteria used to identify the different classes of geomagnetic activity. These criteria are based on daily values of the geomagnetic Aa index and Storm Sudden Commencement (SSC) dates. According to these criteria, recurrent geomagnetic activity is defined by daily values ≥ 40 nT observed for at least two consecutive days and recurring over at least two successive Bartels rotations. The criteria can be represented using pixel diagrams, which are widely employed to visualize and identify the different classes of geomagnetic activity (5, 6, 9). Examples of recurrent events identified using this procedure are shown in Figures 1 and 2. Figure 1 illustrates a recurrent event observed on 21 – 22 September 1996 and recurring on 18 – 19 October 1996, corresponding to recurrent geomagnetic activity over two successive Bartels rotations. Figure 2 shows a more persistent event extending from August to December 2003 and recurring over five successive Bartels rotations.

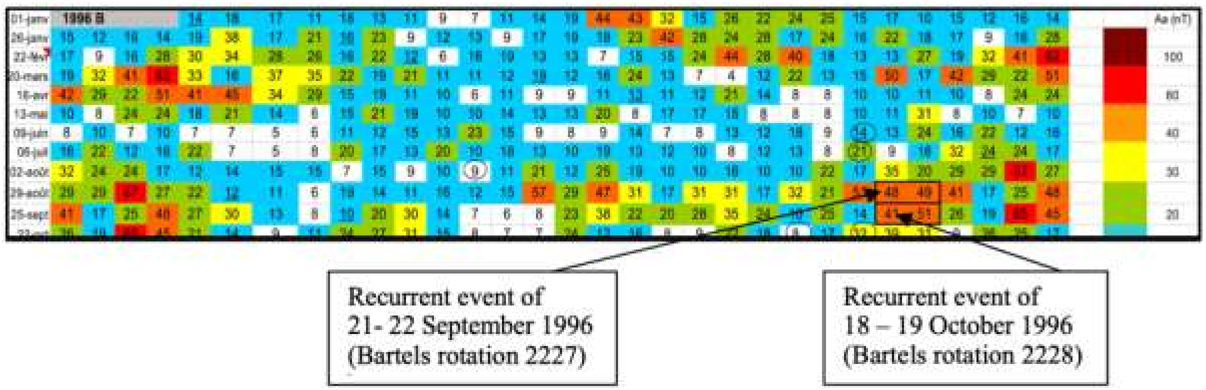

Figure 1: Pixel diagram for 1996. The outlined cells indicate a recurrent geomagnetic activity even observed during two successive Bartels rotations.

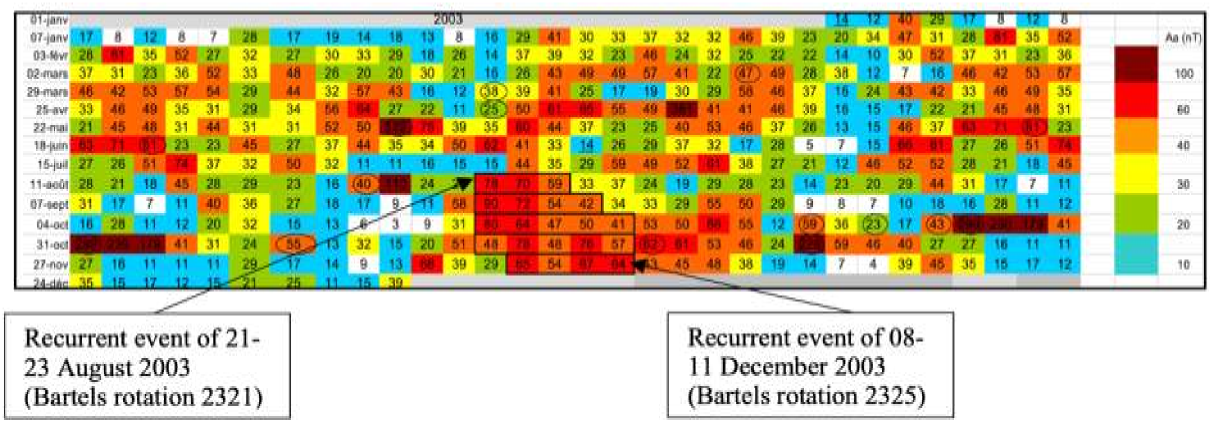

Figure 2: Pixel diagram for 2003. The outlined cells indicate an episode of recurrent geomagnetic activity observed over five successive Bartels rotations.

- **Analysis of solar wind parameters and their relationship with geoeffectiveness:-**

The evolution of solar wind parameters and their relationship with geoeffectiveness during the selected recurrent events was investigated in two stages. First, an individual analysis was performed for each of the 28 recurrent events identified during solar cycles 23 and 24. Subsequently, the Superposed Epoch Analysis (SEA) technique was applied to selected solar wind parameters (22, 23). This method consists of temporally aligning multiple events around a common reference time (t = 0) in order to construct composite profiles representative of the average behavior of the investigated parameters. SEA reduces the influence of event-to-event variability and highlights the characteristic mean signatures of recurrent geomagnetic activity events.

For each event, the analysis window extends from one day before the event onset to one day after its end. This time window allows both the pre-event conditions and the post-event recovery phase to be included in the composite analysis. Moreover, time is defined such that $t = 0$ corresponds to the onset of the event. The onset of a recurrent event is identified as the firsthour of the first day of recurrent geomagnetic activity determined from the pixel diagram. The time $t = n$ corresponds to the end of the event, where n denotes the event duration in hours. For example, $t = 48h$ corresponds to the end of a recurrent geomagnetic event lasting two days. To evaluate the robustness of the trends revealed by the composite profiles, uncertainty bands corresponding to the mean ± standard error of the mean (SEM) were associated with each composite profile. These bands provide information on the dispersion of observations around the mean behavior and allow the inter-event variation to be assessed.

The composite mean was calculated using equation (1):-

$$\bar{x}(t) = \frac{1}{N}\sum_{i=1}^{N} x_i\,(t) \qquad (1)$$

where N is the number of events ($N = 20$) and $x_i(t)$ represents the value of a given parameter at time t for event i. To further quantify the statistical relationships revealed by the composite profiles, Pearson correlation and cross-correlation analyses between each solar wind parameter and the Dst index were subsequently performed. In the cross-correlation analysis, the lag is interpreted as the characteristic time interval separating variations in a solar wind parameter from the corresponding geomagnetic response observed in Dst. Consequently, the lag associated with the maximum cross-correlation coefficient is interpreted as the characteristic response time of Dst to the considered parameter. It should be noted that all correlation coefficients were computed from the composite profiles obtained through the SEA procedure.

The mathematical expressions of the Pearson correlation coefficient and the cross-correlation function are given by Equation (2) and (3), respectively:-

$$r = \frac{\sum_{i=1}^{N}(x_i - \bar{x})(y_i - \bar{y})}{\sqrt{\sum_{i=1}^{N}(x_i - \bar{x})^2} * \sqrt{\sum_{i=1}^{N}(y_i - \bar{y})^2}} \qquad (2)$$

$$R_{xy}(k) = \frac{\sum_{i=1}^{N-k}(x_i - \bar{x})(y_{i+k} - \bar{y})}{\sqrt{\sum_{i=1}^{N}(x_i - \bar{x})^2} * \sqrt{\sum_{i=1}^{N}(y_i - \bar{y})^2}} \qquad (3)$$

where x_i and y_i denote the values of the two variables under consideration (e.g., solar wind speed and Dst index), $\bar{x}$ and $\bar{y}$ their corresponding means, and r the Pearson correlation coefficient, which ranges from -1 to $+1$. Values of r approaching ± 1 indicate a stronger linear relationship. In the cross-correlation analysis, k denotes the temporal lag, and the maximum value of $R_{xy}(k)$ identifies the lag at which the two series are most strongly correlated. Negative lags indicate that variations in the solar wind parameter precede the corresponding variations in Dst, whereas positive lags indicate that Dst variations occur first.

For the SEA analysis, only two-day geomagnetic events were considered, as they represent the dominantcategoryinthe sample (20 out of 28 events) and provide a consistent temporal framework for aligning interplanetary and geomagnetic signatures. The small number of longer recurrent events (3 of three days, 3 of four days, and 2 of five days) is insufficient to produce statistically meaningful results.

- **Geoeffectivenesscriterion:-**

In this study, geoeffectiveness is assessed using the Dst index, which is widely employed as an indicator of geomagnetic storm intensity (15). An event is considered geoeffective when it is associated with a decrease in Dst index reaching at least -30 nT ($Dst_{min} \leq -30$ nT).

Following the classification proposed by (15), geomagnetic storms are categorized according to the minimum Dst value reached during the event:-

- a geomagnetic storm is considered to occur when $Dst_{min} \leq -30\ nT$;
- the storm is classified as weak for $-30\ nT \geq Dst_{min} > -50\ nT$; moderate for $-50\ nT \geq Dst_{min} > -100\ nT$; intense for $-100\ nT \geq Dst_{min} > -200\ nT$ and severe for $-200\ nT \geq Dst_{min} > -350\ nT$

Results:-

Examples of recurrent geomagnetic events:-

Figures 3 and 4 present representative examples of recurrent geomagnetic events identified during solar cycle 23. Figure 3 corresponds to a recurrent geomagnetic activity observed during the solar minimum phase (September – October 1996), whereas Figure 4 illustrates a recurrent geomagnetic activity observed during the declining phase of the cycle (August – December 2003).

The September – October 1996 activity recurred over two consecutive Bartels rotations (2227 and 2228, respectively). In both occurrences, the IMFBz component fluctuated around zero, with several intervals of southward orientation. Unlike most events examined in this study, solar wind speed was already elevated before the onset of the September 1996 event. It gradually decreased during the first day, reached a minimum near the end of the day, and then increased again during the second day to values characteristic of high-speed solar wind streams. Proton density and dynamic pressure remained relatively low throughout event. The geomagnetic response was marked by decreases in the Dst index, with minimum values ranging from $-44\ nT$ to $-52\ nT$. During the October 1996 event, solar wind speed increased rapidly. In less than 12 hours, it rose from ~ 400 to $\sim 600\ km/s$ and it stabilized around $\sim 600\ km/s$ until the end of event. Proton density and dynamic pressure peaked at the beginning of the event before decreasing in the subsequent phase. The Dst underwent a gradual decline from the start of the event. It reached a first minimum of $-42\ nT$ at $t = 6\ h$and a second minimum of $-52\ nT$ at $t = 38h$.

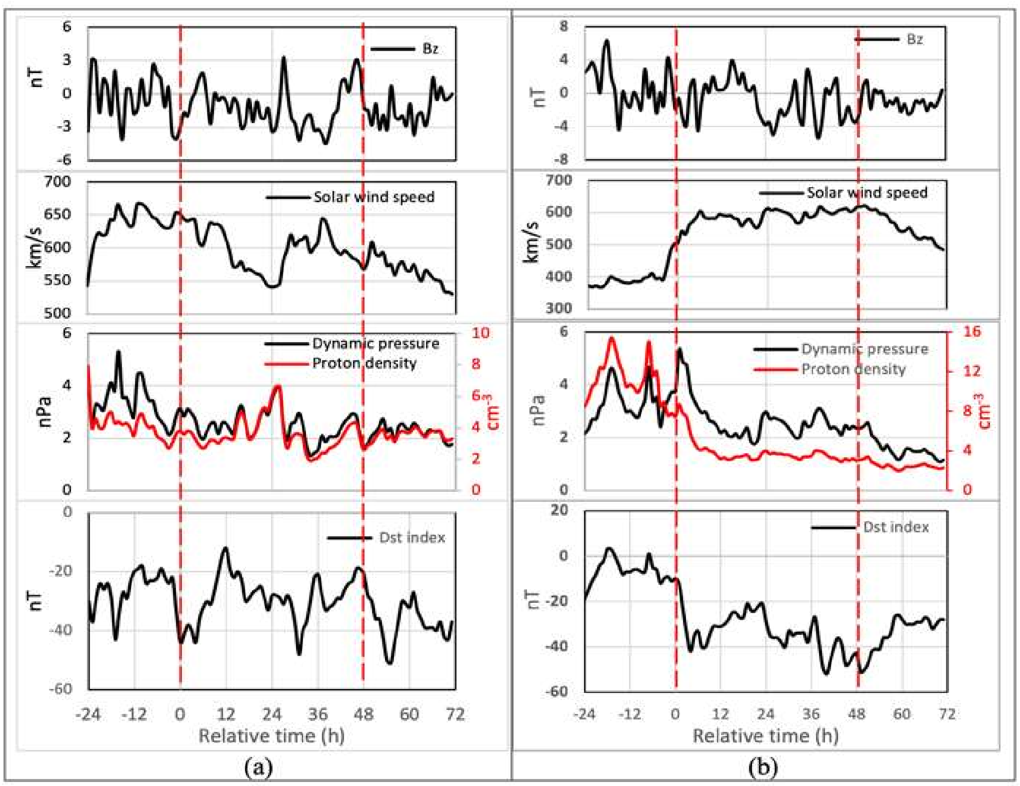

Figure 3: Temporal evolution of the IMF Bz component, solar wind speed, dynamic pressure, proton density, and the Dst index during two recurrent geomagnetic events observed near the minimum phase of Solar Cycle 23. Panel (a) corresponds to the event of 21-22 September 1996 (Bartels rotation 2227), while panel (b) corresponds to the event of 18-19 October 1996 (Bartels rotation 2228). The dashed red lines indicate the beginning and end of each recurrent geomagnetic event.

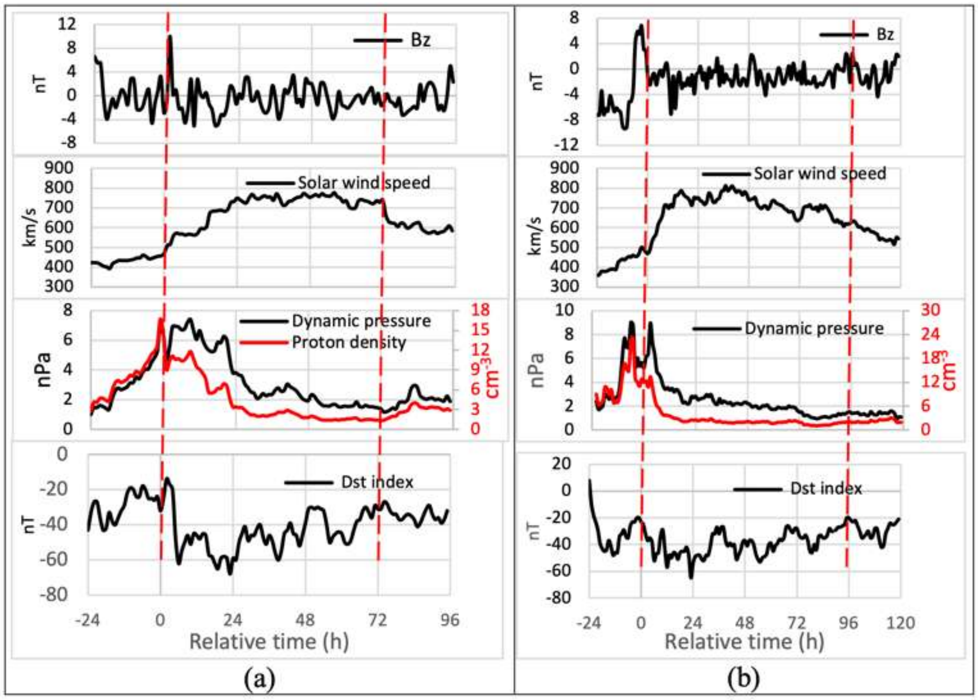

Figure 4: Temporal evolution of the IMF Bz component, solar wind speed, dynamic pressure, proton density, and the Dst index during recurrent geomagnetic events observed the declining phase of Solar Cycle 23. Panel (a) corresponds to the event of 21-23 August 2003 (Bartels rotation 2321), while panel (b) corresponds to the event of 17-20 September 2003 (Bartels rotation 2322). The dashed red lines indicate the beginning and end of each recurrent geomagnetic event.

The August – December 2003 activity persisted over five consecutive Bartels rotations. For brevity, only the first two recurrent events are shown in Figure 4, as the subsequent rotations exhibit similar interplanetary and geomagnetic signatures. Figure 4 presents the first two occurrences (Bartels rotations 2321 and 2322), which lasted three and four days, respectively. Both events were characterized by an initial transition of the IMF Bz component from northward to southward orientation, followed by alternating positive and negative fluctuations. Solar wind speed increased rapidly at the onset of the events, from values typical of slow solar wind ($\sim 400 - 500\ km/s$) to high-speed conditions exceeding 700 km/s. Proton density and dynamic pressure exhibited enhanced values near the beginning of the events before decreasing during the subsequent phase. The geomagnetic response was associated with significant decreases in Dst, reaching minimum values between $-62\ nT$ to $-65\ nT$.

Overall, the recurrent geomagnetic events analyzed in this study exhibit similar temporal characteristics. Prior to event onset, solar wind speed is generally low and relatively stable, while proton density and dynamic pressure tend to increase. The onset phase is characterized by a rapid increase in solar wind speed, a transition of the IMF Bz component toward southward values, and a simultaneous decrease in Dst. During the subsequent phase, solar wind speed remains elevated, whereas proton density and dynamic pressure decrease and stabilize at lower levels. The geomagnetic response is characterized by an initial rapid decrease in Dst followed by a gradual recovery accompanied by fluctuations. These examples illustrate the typical interplanetary and geomagnetic signatures observed during the recurrent events investigated in this study.

Superposed Epoch Analysis (SEA):-

Twenty recurrent geomagnetic events lasting two days were selected for the superposed epoch analysis (SEA), representing 71.43% of all recurrent geomagnetic events identified during solar cycles 23 and 24.

Figure 5 presents the composite profiles of solar wind parameters and the Dst index. Solar wind speed exhibits a progressive increase from approximately $430\ km/s$ at the event onset to about $620\ km/s$ at $t = 48\ h$, with a maximum near $640\ km/s$ around $t = 36\ h$. After the event, the speed gradually decreases. Proton density shows a moderate enhancement near the beginning of the event before progressively decreasing during the main phase. Dynamic pressure remains relatively low but displays a slight increase near the onset. The IMF Bz component fluctuates around zero, with a tendency toward negative values during the central phase of the event. The Dst index progressively decreases after event onset and reaches a minimum value close to $-50\ nT$ around $t \approx 26\ h$.

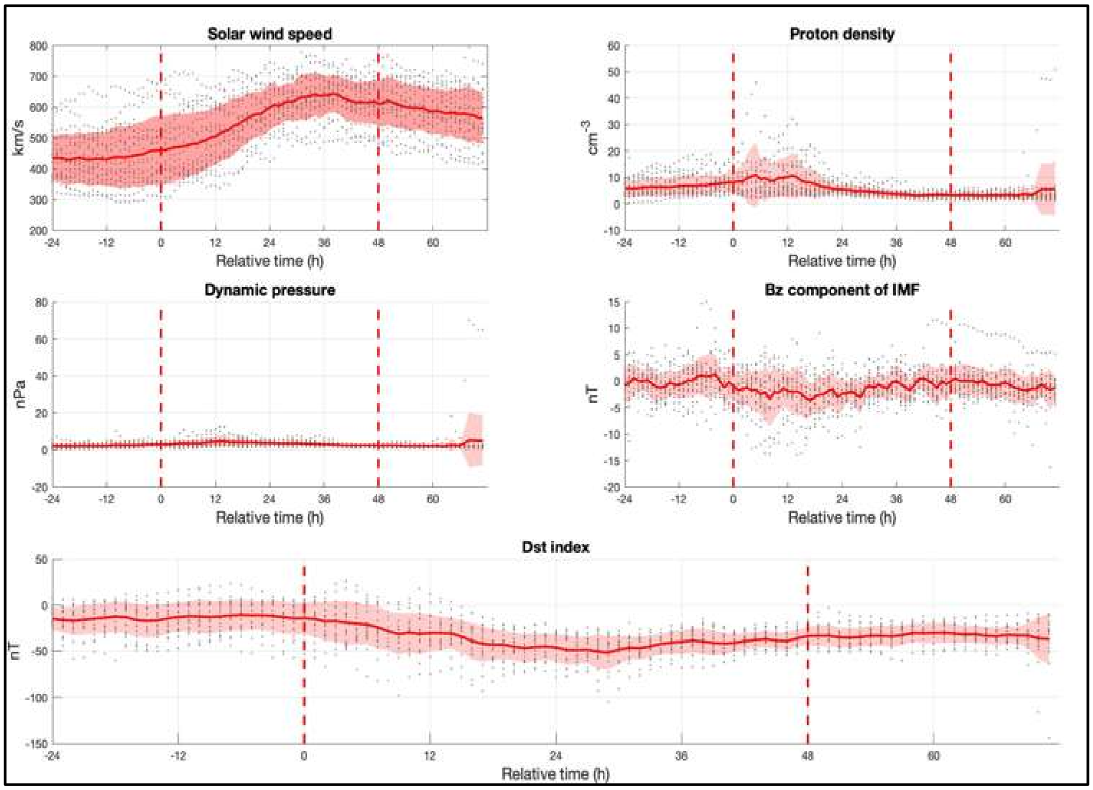

Figure 5: Superposed epoch analysis (SEA) of 20 recurrent geomagnetic events lasting two days. Panels show the composite profiles of solar wind speed, proton density, dynamic pressure, IMF Bz component in GSM coordinates, and the Dst index. The solid red curves represent the mean composite profiles, while the shaded red areas indicate the uncertainty bands (mean ± SEM). Gray dots correspond to the individual event values used in the analysis. The dashed red lines indicate the beginning ($t = 0\ h$) and end ($t = 48\ h$) of the recurrent geomagnetic events.

Tables 1 and 2 and Figure 6 summarize the linear and cross-correlation analyses between solar wind parameters and Dst. The strongest linear correlation is observed between solar wind speed and Dst ($r = -0.894$). More moderate correlations are found for proton density, dynamic pressure and IMF Bz. Cross-correlation analysis reveals characteristic lags of approximately $-40\ h$ for solar wind speed, $-8\ h$ for IMF Bz, $+16\ h$ for proton density, and $+23\ h$. for dynamic pressure relative to Dst.

Table 1: Pearson correlation coefficients between composite solar wind parameters and the composite Dst index derived from the SEA of 20 recurrent two-day geomagnetic events.

Solar wind parameters	Pearson correlation coefficient (r)
Speed	– 0.894
Proton density	+ 0.459
Dynamic pressure	– 0.391
IMF Bz component	+ 0.444

Table 2: Strongest coefficients obtained with the cross-correlation functions between composite solar wind parameters and the composite Dst index obtained from the SEA of 20 recurrent two-day geomagnetic events, as well as the corresponding time lag.

Solar wind parameters	Maximum correlation	Time lag (hours)
Speed	+ 0.459	– 40
Proton density	+ 0. 914	+ 16
Dynamic pressure	+ 0. 594	+ 23
IMF Bz component	+0. 586	– 8

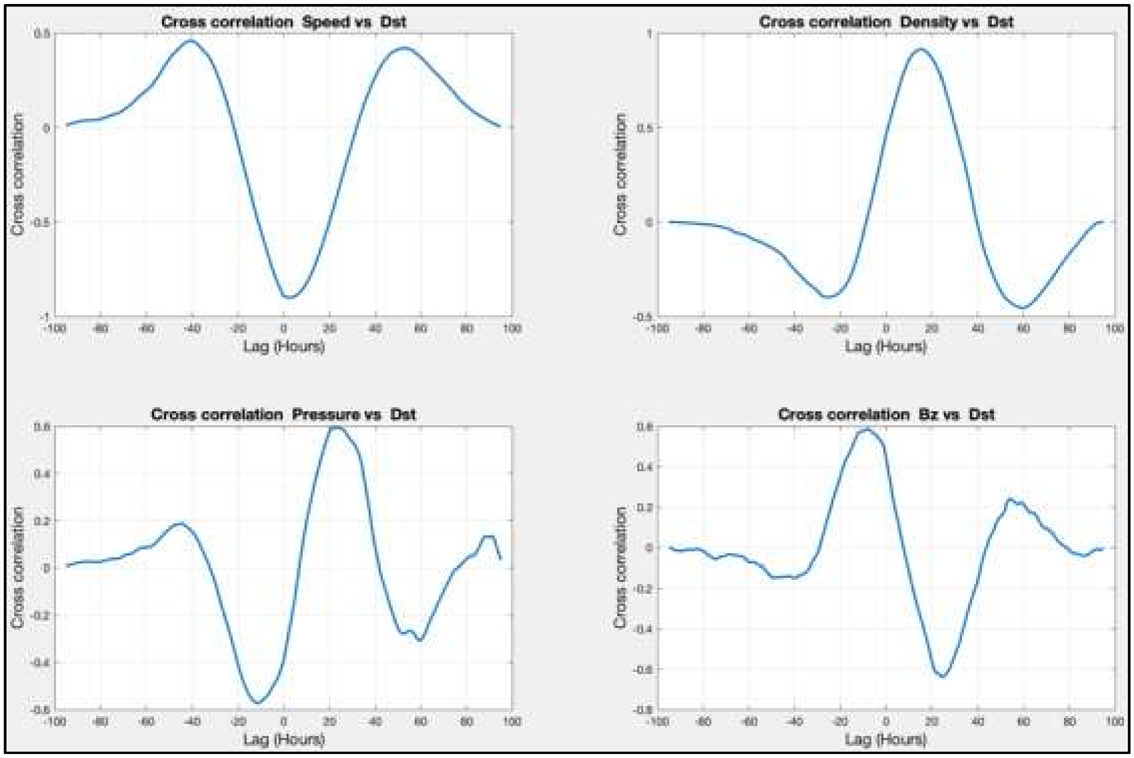

Figure 6: Cross-correlation functions between composite solar wind parameters and the composite Dst index obtained from the superposed epoch analysis of 20 recurrent two-day geomagnetic events.

Discussion:-

The recurrent geomagnetic events analyzed in this study exhibit interplanetary signatures characteristic of high-speed solar wind streams and stream interaction regions (SIRs/CIRs). The recurrence of these events over successive Bartels rotations suggests an association with long-lived coronal holes, which can persist for several solar rotations and are recognized as the primary sources of recurrent high-speed solar wind streams (24, 25, 26). The observed increase in solar wind speed, together with the subsequent enhancements in proton density and dynamic pressure, are consistent with the compression plasma regions commonly observed in CIR structures (26, 27).

The individual event analysis and the composite profiles obtained from the superposed epoch analysis indicate that several solar wind parameters contribute to the geoeffectiveness of recurrent geomagnetic activity through complementary physical mechanisms . Solar wind speed exhibits the strongest overall relationship with the Dst index, as evidenced by the strong Pearson correlation coefficient obtained from the composite profile. This result supports the view that high-speed streams are the primary drivers of recurrent geomagnetic activity, in agreement with previous studies (28, 29). However, the occurrence of geomagnetic disturbances also depends on the orientation of the interplanetary magnetic field. The recurrent southward Bz intervals observed near event onset likely promote magnetic reconnection at the magnetopause and facilitate the transfer of solar wind energy into the magnetosphere (15, 30). The enhancements in proton density and dynamic pressure observed at the beginning of the events are characteristic of the compressed plasma regions associated with CIRs and contribute to strengthening the magnetospheric response.

The geomagnetic response is characterized by decreases in Dst ranging from approximately $-40\ nT$ to $-90\ nT$, indicating predominantly weak to moderate geomagnetic storms conditions according to the classification of (15). These amplitudes are characteristic of CIR-driven storms, which are generally less intense than CME-driven storms but occur more frequently during periods dominated by long-lived coronal holes (28, 31). The moderate intensity of the observed disturbances may be related to the relatively short duration of the southward Bz intervals identified during the events.

The cross-correlation analysis provides additional insight into the temporal relationships between solar wind parameters and the geomagnetic response. The lag of approximately 40 h between solar wind speed and Dst indicates that variations in solar wind speed precede the geomagnetic response and therefore act as an important precursor of recurrent geomagnetic activity. In contrast, the shorter lag observed for the IMF Bz component (approximately 8 h) suggests a more direct influence on storm development through magnetic reconnection. Proton density and dynamic pressure exhibit significant cross-correlations with Dst, particularly proton density, which presents the highest maximum cross-correlation coefficient. However, the positive lags associated with these parameters suggest that they primarily modulate the intensity of the geomagnetic response through plasma compression processes rather than directly triggering geomagnetic activity. The consistency between the individual-event analysis and the superposed epoch analysis strengthens the robustness of the interpretations and highlights the complementary roles of solar wind speed, IMF orientation, and plasma compression in controlling the geoeffectiveness of recurrent geomagnetic events.

Conclusion:-

This study identified and characterized 28 recurrent geomagnetic events observed during solar cycles 23 and 24. The analysis of solar wind parameters indicates that these events are primarily associated with high-speed streams originating from long-lived coronal holes and the corresponding stream/corotating interaction regions (SIRs/CIRs). The observed signatures include an increase in solar wind speed, compression of the interplanetary plasma, and the occurrence of southward Bz intervals favorable to energy transfer into the magnetosphere.

The superposed epoch analysis, combined with linear and cross-correlation analyses, shows that solar wind speed is the parameter most strongly associated with the overall evolution of Dst, whereas the IMF Bz component plays a key role in triggering the geomagnetic response. Proton density and dynamic pressure mainly contribute to modulating the intensity of this response through compression processes associated with CIRs.

The disturbances observed correspond predominantly to weak-to-moderate geomagnetic storms, confirming that CIRs constitute an important source of recurrent geoeffectiveness during solar cycles 23 and 24. These results contribute to a better understanding of Sun-Earth coupling processes associated with recurrent events and highlight the relevance of solar wind parameters for geomagnetic activity forecasting. It should nevertheless be noted that these findings are constrained by the relatively small number of events analyzed and by the restriction to two-day events across two Bartels rotations.

Data available statement:-

The results presented in this manuscript are based on freely accessible data (Solar wind parameters and geomagnetic indexes) from the OMNI and ISGI websites, whose addresses are respectively https://omniweb.gsfc.nasa.gov/hw.html et https://isgi.unistra.fr/data_download.php

Conflicts of interest:-

The authors declare no conflicts of interest.

Funding:-

The authors declare that they have received no funding for this manuscript.

Acknowledgement:-
We thank the use of NASA/GSFC's Space Physics Data Facility OMNIWeb service and OMNI data. We also thank the International Service of Geomagnetic Indices (ISGI) and collaborating institutes for providing geomagnetic indices.

References:-
1. Gauss, C.F. (1833). Intensitas vis magneticaeterrestrisadmensuramabsolutamrevocata. CommentationesSocietatisRegiaeScientiarumGottingensisRecentiores, 8, 3-44.
2. Sabine, E. (1846). Contributions to terrestrial magnetism. No. VII. Philosophical Transactions of the Royal Society of London, 136, 237-336.
3. Sabine, E. (1856). On periodical laws discoverable in the mean effects of the larger magnetic disturbances. No. III. Philosophical Transactions of the Royal Society, 146, 357-374.
4. Zerbo, J. L., Ouattara, F., Zoundi, C., &Gyébré, A. M. F. (2011). Cycle solaire 23 et activitégéomagnétiquedepuis 1868. Revue CAMES, Série A, 12, 255 – 262.
5. Legrand, J.-P., & Simon, P. A. (1989a). Solar cycle and geomagnetic activity: A review for geophysicists. Part I. The contributions to geomagnetic activity of shock waves and of the solar wind. Annales Geophysicae, 7, 565-578.
6. Legrand, J.-P., & Simon, P. A. (1989b). Solar cycle and geomagnetic activity: A review for geophysicists. Part II. The solar sources of geomagnetic activity and their links with sunspot cycle activity. Annales Geophysicae, 7, 579-594.
7. Mayaud, P.N. (1973). A hundred year series of geomagnetic data, 1868-1967: Indices-aa, storm sudden commencements. IAGA Bulletin No. 33.
8. Richardson, I. G., Cliver, E. W., & Cane, H. V. (2000). Sources of geomagnetic activity over the solar cycle: Relative importance of coronal mass ejections, high-speed streams, and slow solar wind. Journal of Geophysical Research: Space Physics, 105(A8), 18203-18213. https://doi.org/10.1029/1999JA000400
9. Ouattara, F., & Amory-Mazaudier, C. (2009). Solar–geomagnetic activity and aa indices toward a standard classification. Journal of Atmospheric and Solar–Terrestrial Physics, 71(17-18), 1736-1748. https://doi.org/10.1016/j.jastp.2008.05.001
10. Zerbo, J. L., Amory-Mazaudier, C., Ouattara, F., & Richardson, J. D. (2012). Solar wind and geomagnetism: Toward a standard classification of geomagnetic activity from 1868 to 2009. Annales Geophysicae, 30(3), 421-426. https://doi.org/10.5194/angeo-30-421-2012
11. Zerbo, J. L., Amory-Mazaudier, C., &Ouattara, F. (2015). On solar wind speed distribution and geomagnetic activity during solar cycle 23. International Journal of Physical Sciences, 10(21), 562-567. https://doi.org/10.5897/IJPS2015.4401
12. Zhang, J., Richardson, I. G., Webb, D. F., et al. (2007). Solar and interplanetary sources of major magnetic storms (Dst ≤ -100 nT) during 1996–2005. Journal of Geophysical Research: Space Physics, 112(A10), A10102. https://doi.org/10.1029/2007JA012321
13. Richardson, I. G., & Cane, H. V. (2010). Near-Earth interplanetary coronal mass ejections during solar cycle 23 (1996-2009): Catalog and Summary of Properties. Solar Physics, 264, 189-237. https://doi.org/10.1007/s11207-010-9568-6
14. Yan, P., Li, X., Zheng, Y. et al. (2024). A real-time solar flare forecasting system with deep learning methods. Astrophysics and Space Science, 369, 110. https://doi.org/10.1007/s10509-024-04374-8
15. Gonzalez, W. D., Joselyn, J. A., Kamide, Y., et al.(1994). What is a geomagnetic storm? Journal of Geophysical Research: Space Physics, 99(A4), 5771-5792. https://doi.org/10.1029/93JA02867
16. 16.Tsurutani, B. T., & Gonzalez, W. D. (1997). The interplanetary causes of magnetic storms: A review. In B. T. Tsurutani, W. D. Gonzalez, Y. Kamide, & J. Kroehl (Eds.), Magnetic Storms (pp. 77-89). American Geophysical Union. https://doi.org/10.1029/gm098p0077
17. Akasofu, S.-I. (2021). A review of studies of geomagnetic storms and auroral/magnetospheric substorms based on the electric current approach. Frontiers in Astronomy and Space Sciences, 7, 604750. https://doi.org/10.3389/fspas.2020.604750
18. Gopalswamy, N., Akiyama, S., Yashiro, S., et al.(2025). Annotated catalog of intense geomagnetic storms including their solar and interplanetary causes. Journal of Astrophysics and Astronomy, 46, 78. https://doi.org/10.1007/s12036-025-10091-7
19. King, J. H., &Papitashvili, N. E. (2005). Solar wind spatial scales in and comparisons of hourly Wind and ACE plasma and magnetic field data. Journal of Geophysical Research: Space Physics, 110(A2), A02104. https://doi.org/10.1029/2004JA010649

20. Weimer, D. R., Ober, D. M., Maynard, N. C., et al.(2002). Variable time delays in the propagation of the interplanetary magnetic field. Journal of Geophysical Research: Space Physics, 107(A8), 1210. https://doi.org/10.1029/2001JA009102
21. Legrand, J.-P., & Simon, P. A. (1981). Ten cycles of solar and geomagnetic activity. Solar Physics, 70(1), 173-195. https://doi.org/10.1007/BF00154399
22. Chree, C. (1913). Some phenomena of sunspots and of terrestrial magnetism at Kew Observatory. PhilosophicalTransactions of the Royal Society A: Mathematical, Physical and Engineering Sciences, 212(484-496), 75–116.https://doi.org/10.1098/rsta.1913.0003
23. Singh, Y. P., &Badruddin. (2006). Statistical considerations in superposed epoch analysis and its applications in space research. Journal of Atmospheric and Solar-Terrestrial Physics, 68(7), 803-813. https://doi.org/10.1016/j.jastp.2006.01.007
24. Krieger, A. S., Timothy, A. F., &Roelof, E. C. (1973). A coronal hole and its identification as the source of a high velocity Solar wind stream. Solar Physics, 29(2), 505-525.https://doi.org/10.1007/BF00150828
25. Cranmer, S. R. (2009). Coronal holes. Living Reviews in Solar Physics, 6, 3. https://doi.org/10.12942/lrsp-2009-3
26. Richardson, I. G. (2018). Solar wind stream interaction regions throughout the heliosphere. Living Reviews in Solar Physics, 15, Article 1. https://doi.org/10.1007/s41116-017-0011-z
27. Jian, L., Russell, C. T., Luhmann, J. G., et al.(2006). Properties of Interplanetary Coronal Mass Ejections at One AU During 1995-2004. Solar Physics,239, 393-436. https://doi.org/10.1007/s11207-006-0133-2
28. Tsurutani, B. T., & Gonzalez, W. D. (1995). The future of geomagnetic storm predictions: Implications from recent solar and interplanetary observations. Journal of Atmospheric and Terrestrial Physics, 57, 1369-1384. https://doi.org/10.1016/0021-9169(95)00138-R
29. Tsurutani, B. T., Gonzalez, W. D., Gonzalez, A. L. C., et al. (2006). Corotating solar wind streams and recurrent geomagnetic activity: A review, Journal of Geophysical Research., 111, A07S01. https://doi.org/10.1029/2005JA011273
30. Dungey, J. W. (1961). Interplanetary magnetic field and the auroral zones. Physical Review Letters, 6(2), 47-48. https://doi.org/10.1103/PhysRevLett.6.47
31. Richardson, I. G., & Cane, H. V. (2012). Near-Earth solar wind flows and related geomagnetic activity during more than four solar cycles (1963-2011). Journal of Space Weather and Space Climate, 2, A02. https://doi.org/10.1051/swsc/2012003